The International Journal of Cardiovascular Imaging (2019) 35:1627–1636
https://doi.org/10.1007/s10554-019-01612-x

ORIGINAL PAPER

Effect of diastolic dysfunction on intraventricular velocity behavior in early diastole by flow mapping

Bostjan Berlot[1,2] · Jose Luis Moya Mur[1] · Borut Jug[2] · Daniel Rodríguez Muñoz[1] · Alicia Megias[1] · Eduardo Casas Rojo[1] · Covadonga Fernández-Golfín[1] · Jose Luis Zamorano[1]

Received: 11 December 2018 / Accepted: 25 April 2019 / Published online: 30 April 2019

Abstract
Intraventricular velocity distribution reflects left ventricular (LV) diastolic function and can be measured non-invasively by flow mapping technologies. We designed our study to compare intraventricular velocities and gradients, obtained by vector flow mapping (VFM) technology during early diastole in consecutive patients diagnosed with mild and advanced diastolic dysfunction at echocardiography and a control group with a purpose to validate the hypothesis of relationship between new parameters and severity of diastolic dysfunction and conventional markers of elevated LV filling pressure. Two-dimensional streamline fields were obtained using VFM technology in 121 subjects (57 with normal diastolic function, 38 with mild diastolic dysfunction and 26 with advanced diastolic dysfunction). We measured several velocities and calculated a gradient along the selected streamline, which we compared between groups and correlated them with conventional echocardiographic parameters. Apical intraventricular velocity gradient (Gr_{IV}) was the lowest in control group, followed by mild and advanced diastolic dysfunction groups (5.3 ± 1.9 vs. 6.8 ± 2.5 vs. 13.6 ± 5.0/s, $p < 0.001$) and showed good correlation with E/e' ($r = 0.751$, $p < 000.1$). Gr_{IV}/e' ratio was the strongest single predictor of severity of diastolic dysfunction. Different degrees of diastolic dysfunction affect the Intraventricular velocity behavior during early diastole obtained by VFM. Gr_{IV} could discriminate between groups with different levels of diastolic dysfunction and was closely associated with classical echocardiographic indices of elevated LV filling pressure. Gr_{IV}/e' ratio has a potential to become a single parameter needed to assess left ventricular diastolic function.

Keywords Diastolic dysfunction · Echocardiography · Intraventricular velocity gradient · Vector flow mapping · Blood flow dynamics

Introduction

Left ventricular (LV) diastolic filling is affected by several factors, such as ventricular relaxation, suction, chamber compliance, left atrial (LA) pressure, cardiac preload and afterload. Lack of a single-point echocardiographic measurement and a complex non-uniform nature of the LV filling pattern, make the assessment of diastolic function challenging [1, 2]. Moreover, some studies have demonstrated the limited accuracy of conventional Doppler-derived parameters [3]. There is a strong clinical need to identify and understand abnormalities of LV filling dynamics since they indicate a group with higher risk for hospitalization and mortality [4, 5].

At the LV chamber level, diastole is a continuous interplay between elastic recoil forces and relaxation forces relative to the load encountered [6, 7]. Through early rapid filling they generate intraventricular pressure gradients that result in transmitral flow (E wave) linked to formation of vortex ring in the LV. Vortex ring appears in three-dimensional view as a closed tube with torus-like shape and can be observed by flow mapping technologies as a counter-rotating vortex pair with a virtual hydrodynamic channel, believed

This author takes responsibility for all aspects of the reliability and freedom from bias of the data presented and their discussed interpretation.

✉ Bostjan Berlot
bostjan.berlot@gmail.com

[1] Cardiology Department, Hospital Universitario Ramon y Cajal, de km. 9, 100, Ctra. Colmenar Viejo, 28034 Madrid, Spain

[2] Faculty of Medicine, University of Ljubljana, Vrazov trg 2, 1000 Ljubljana, Slovenia

to help rapid mass transport from the atrium to LV apex [8]. Some trials have demonstrated association between base-to-apex flow velocity distribution measured by colour M-mode, increased LV filling pressures and diastolic dysfunction [9–12]. However, this 1-dimensional scanning technique has several limitations due to the lack of information on spatial distribution [13].

Vector flow mapping (VFM) is an emerging technology fusing Doppler and speckle tracking information to display 2-dimensional flow velocity vector field in vascular structures without angle dependency [14]. It can provide information on intraventricular velocity distribution during diastole along the base-to-apex streamlines. The accuracy of the velocity vector field derived from VFM has been validated by computer-simulated phantom [15]. We designed our study to compare intraventricular velocities and gradients, obtained by VFM technology during early diastole in consecutive patients diagnosed with mild diastolic dysfunction (MDD) and advanced diastolic dysfunction (ADD) at echocardiography and a control group with a purpose to validate the hypothesis of relationship between new parameters and severity of diastolic dysfunction and conventional markers of elevated LV filling pressure.

Methods

Study population

One hundred and twenty-one patient referred for echocardiographic evaluation of cardiac function between December 2015 and May 2016 was studied. Inclusion criteria for the study population were adequate image quality, LV ejection fraction (EF) above 55%, sinus rhythm with heart rate (HR) below 95 bpm, absence of more than mild aortic or mitral native valve disease and absence of prosthetic valves. Subjects were divided into three groups following the algorithm proposed in the current echocardiography guidelines for LV diastolic function evaluation [2]. In the first group, there were 38 consecutive subjects diagnosed with mild diastolic dysfunction (impaired relaxation pattern on trans-mitral pulsed Doppler examination, E/e' ratio < 14, absence of pulmonary hypertension and mildly dilated LA). Second group, consisted of 26 subjects with moderate and severe diastolic dysfunction (pseudo-normal pattern on trans-mitral pulsed Doppler, pulmonary hypertension, severely enlarged LA and low mitral annulus tissue Doppler velocities) and control group, where 57 consecutive patients free of heart failure symptoms, without echocardiographic signs of structural disease, referred to echocardiography without heart failure suspicion, met criteria for normal diastolic function according to ESC guidelines. The study was approved by institutional review board, and all participants provided written informed consent.

Image acquisition

Echocardiographic examination was performed using a 3.5–5.0 MHz probe and a ProSound F75 CV Premier diagnostic ultrasound system (Hitachi-Aloka Ltd., Tokyo, Japan) with subjects in standard left lateral semi-recumbent position. Diastolic function was assessed in the apical 4-chamber view by measuring conventional parameters: E wave (E) and A wave velocity (A), E/A ratio, indexed left atrium volume (LAVI) and tricuspid regurgitation (TR) velocity, following current recommendations for diastolic function assessment [2]. LV end-diastolic diameter, intra-ventricular septum, posterior wall and end-systolic LV diameter were measured in parasternal long-axis view from which mass (LV mass) and ejection fraction (LV EF) were calculated by linear method after ruling out regional wall motion abnormalities or systolic dysfunction. Pulsed-wave tissue Doppler spectrograms from the septal and lateral mitral annulus were averaged (e') and used to calculate E/e' ratio.

Parameters and vector flow mapping processing

A video clip of three consecutive beats with time resolution above 30 fps in apical long-axis view with 2D colour Doppler sector fully covering the LV chamber was analysed offline using dedicated VFM software (DAS-RS1, Hitachi-Aloka Medical, Tokyo). Fusing speckle tracking and colour Doppler information the software first created 2D velocity vector field and then transformed it into streamlines (Fig. 1).

We selected the frame with the highest velocity (close to peak E wave) and searched for the streamline (usually the most central one) with the highest velocity (Fig. 2a). Software then displayed velocity distribution along the selected streamline in a velocity over length chart where we measured: velocity at the mitral annulus level (V_{base}), velocity at the entrance of the vortex ring (V_{enter}), maximum velocity, normally located in centre of vortex ring (V_{max}), velocity at the exit of the vortex ring (V_{exit}) and velocity at the 75% of LV length (V_{apex}) (Fig. 2b). We used V_{exit} and V_{apex} to get apical intraventricular velocity gradient (Gr_{IV}).

Statistical analysis

Variables are described as mean ± SD using statistical software IBM SPSS (version 23). Quantitative variables were compared using Student t tests for intergroup comparisons and one-way analysis of variance (ANOVA) for intragroup comparisons. When analysis revealed a significant difference a post hoc comparison test was performed with Bonferroni's test. We studied correlation of VFM

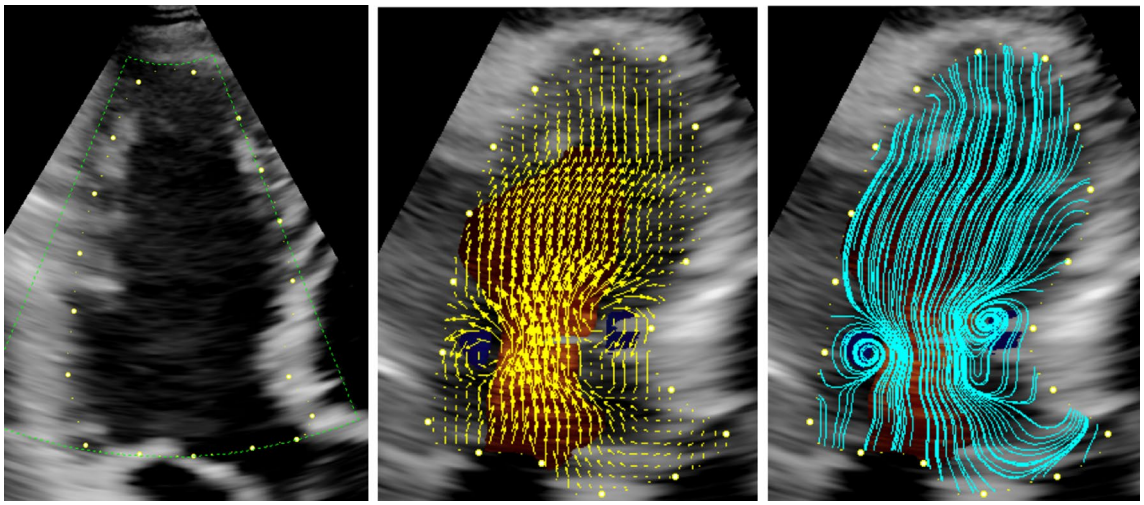

Fig. 1 Overview of the methods used for image acquisition and processing for the study. Speckle tracking white dots and green color Doppler sector (left) used to create 2D vector field (center), which was converted into base-to-apex streamlines (right)

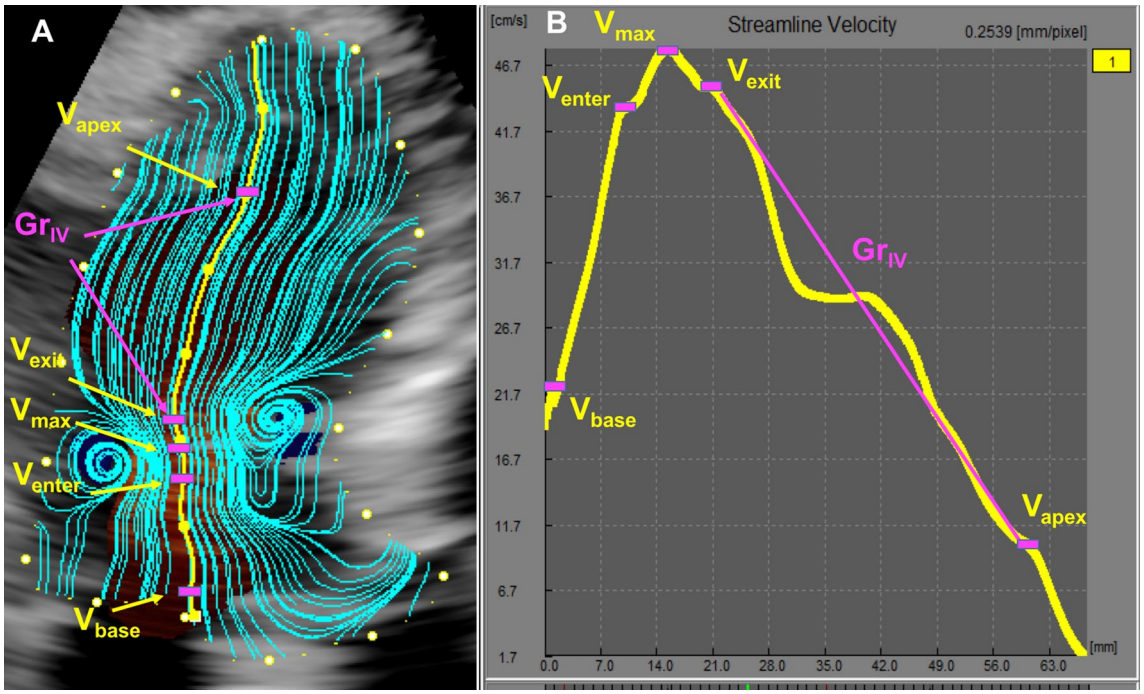

Fig. 2 **a** Left ventricle in streamline view with marked locations (arrows) where we measured velocities and calculated intraventricular velocity gradient (Gr_{IV}) on selected central streamline (yellow line). **b** Selected streamline represented as a velocity over length chart where measured velocities and Gr_{IV} could be identified

parameters using Pearson linear correlation analysis, multivariate and univariate linear regression to study significant predictors of LV filling pressure and ordinal logistic regression to assess association of different parameters with the grade of severity of diastolic dysfunction. To test intraobserver variability main investigator repeated the measurements of 10 randomly selected cases. Same cases were then independently measured by other observer to test interobserver variability. Intraobserver and interobserver agreements were calculated using intra-class correlation coefficient (ICCs) with excellent agreement defined as ICC > 0.8. Statistical significance was established at $p < 0.05$ level.

Results

Study group and conventional echocardiographic parameters

Clinical profile of study group and conventional echocardiographic parameters are shown in Table 1. Patients with diastolic dysfunction were significantly older than controls. There was no major difference between groups in terms of demographic characteristics, except patients with ADD had lower HR ($p=0.038$) and higher systolic blood pressure ($p=0.036$) compared to control group. All subjects in the control group were NYHA I, whereas 32% of patients in MDD and 65% in ADD group were NYHA II or higher. LV ejection fraction and end-diastolic diameter were within normal range and not significantly different. Groups were significantly different in all conventional parameters used to describe LV diastolic function and LV filling pressures.

Intraventricular velocity distribution

All measured intraventricular velocities and calculated gradient along the streamline differ significantly between groups (Table 2). Post hoc analyses showed that V_{enter}, V_{max}, V_{exit} and calculated Gr_{IV} could discriminate between all three groups ($p<0.05$), whereas V_{base} was not significantly different between MDD and control group ($p=0.072$, $p=0.217$). V_{apex} was different only between MDD and ADD group ($p=0.014$) and could not discriminate between control and other two groups.

Table 2 Results of intraventricular velocities and apical intraventricular gradient

	Control group	MDD	ADD	p
V_{base} (cm/s)	31.4 ± 14.2	23.5 ± 10.8	40.9 ± 24.4	< 0.001
V_{enter} (cm/s)	37.9 ± 12.5	30.4 ± 9.12	51.8 ± 22.1	< 0.001
V_{max} (cm/s)	50.8 ± 20.3	38.0 ± 12.5	77.4 ± 31.1	< 0.001
V_{exit} (cm/s)	34.5 ± 8.1	30.3 ± 7.9	57.1 ± 18.1	< 0.001
V_{apex} (cm/s)	13.0 ± 5.3	10.3 ± 4.9	14.4 ± 6.9	0.011
Gr_{IV} (1/s)	5.3 ± 1.9	6.8 ± 2.5	13.6 ± 5.0	< 0.001

Values are mean ± SD

ADD advanced diastolic dysfunction, *enter* at the entrance into the vortex, *exit* at the exit of the vortex, Gr_{IV} apical intraventricular gradient, *max* maximal velocity, *MDD* mild diastolic dysfunction, *V* velocity

Table 1 Demographic characteristics and conventional echocardiographic parameters

	Control group	MDD	ADD	p
n	57	38	26	
Age (years)	50.8 ± 14.2	72.5 ± 12.6	74.0 ± 12.0	< 0.001
Sex (M %/F %)	50/50	55/45	61/39	0.609
Height (cm)	167.0 ± 9.6	163.8 ± 8.9	163.4 ± 8.4	0.074
Weight (kg)	74.3 ± 21.24	71.8 ± 13.16	77.3 ± 15.7	0.486
Heart Rate (bpm)	68 ± 10.9	72 ± 11.9	65 ± 11.3	0.038
Systolic Blood Pressure (mmHg)	134 ± 16.1	144 ± 23.9	140 ± 18.1	0.036
Diastolic Blood Pressure (mmHg)	79 ± 12.3	77 ± 16.0	74 ± 12.2	0.352
NYHA				
I (n, %)	57 (100)	26 (68)	9 (35)	
≥ II (n,%)	0 (0)	12 (32)	17 (65)	< 0.001
LV EF %	72.2 ± 8.1	67.9 ± 9.0	69.5 ± 8.6	0.047
LV EDd (cm)	4.5 ± 0.5	4.3 ± 0.6	4.3 ± 0.7	0.104
Indexed LV mass (g/m^2)	76.2 ± 19.8	93.5 ± 25.0	110.8 ± 44.0	< 0.001
LAVI (ml/m^2)	29.3 ± 8.9	37.3 ± 13.8	47.8 ± 18.7	< 0.001
Peak E wave velocity (cm/s)	74.3 ± 16.9	62.2 ± 13.8	107.8 ± 28.6	< 0.001
Peak A wave velocity (cm/s)	63.6 ± 13.9	91.4 ± 17.2	76.4 ± 23.8	< 0.001
E/A velocity ratio	1.2 ± 0.3	0.7 ± 0.15	1.6 ± 0.80	< 0.001
e' (cm/s)	12.1 ± 2.7	8.3 ± 2.3	6.5 ± 1.5	< 0.001
E/e' ratio	6.4 ± 1.8	7.8 ± 2.2	17.9 ± 7.4	< 0.001
TR velocity (cm/s)	2.3 ± 0.2	2.6 ± 0.4	3.0 ± 0.5	< 0.001

Values are n, mean ± SD, or n (%)

A peak A wave velocity, *ADD* advanced diastolic dysfunction, *E* Peak E wave velocity *e'* average mitral annulus velocity, *EDd* end-diastolic diameter, *EF* ejection fraction, *LAVI* indexed left atrium volume, *LV* left ventricle, *MDD* mild diastolic dysfunction, *NYHA* New York Heart Association, *TR* tricuspid regurgitation

Velocities closer to the base of LV (V_{base}, V_{enter}, V_{max}) showed the strongest correlation to the peak E wave velocity (r = 0.560, r = 0.607, r = 0.716, p < 0.001), but did not correlate with e' and correlate fairly with other conventional parameters used to assess LV diastolic function. V_{exit} showed the strongest correlation with indices of LV filling pressure E/e' and TR velocity (r = 0.709 and r = 0.660, p < 0.001), whereas V_{apex} correlated poorly with conventional diastolic dysfunction parameters. Calculated Gr_{IV} parameter was associated to all conventional parameters, showing the strongest correlation with E/e' (r = 0.751, p < 0.001) and weakest correlation with e' (r = −0.447, p < 0.001) (Table 3).

Univariate logistic regression of new VFM parameters used to categorize cases according to the grade of diastolic dysfunction showed that Gr_{IV} was the best single independent predictor (Table 4) and had the strongest correlation with established indices of LV filling pressure. Gr_{IV} could explain the highest percentage of E/e' variability in simple linear regression analysis (R^2 = 0.560, p < 0.001), but it was weakly associated to e', hence we used this conventional parameter of LV relaxation to create Gr_{IV}/e' ratio.

Inter- and intraobserver variability

Intraobserver paired sample correlations and ICCs showed excellent agreement for intraventricular velocity gradient (Gr_{IV}). ICC = 0.974 (95% CI 0.912–0.992), r = 0.980 p < 0.001. Correlations and ICCs between two observers were: ICC = 0.955 (95% CI 0.853–0.987) and r = 0.972 p < 0.001.

Discussion

This study has demonstrated: (i) the ability of flow mapping technique to discriminate between levels of diastolic dysfunction based on distribution of intraventricular velocities, (ii) a direct relationship between intraventricular velocity gradient, left ventricular filling pressure and level of diastolic dysfunction and (iii) a potential power of newly proposed GR_{IV}/e' parameter to describe the grade of diastolic dysfunction as a single independent parameter.

Table 4 Vector flow mapping parameters as predictors of severity of diastolic dysfunction

	Univariate ordinal regression			
	Pseudo-R^2	Estimate	p	95% CI
V_{base}	0.016	0.014	0.173	−0.006–0.033
V_{enter}	0.056	0.028	0.012	0.006–0.050
V_{max}	0.088	0.023	0.002	0.009–0.037
V_{exit}	0.243	0.073	< 0.001	0.043–0.102
V_{apex}	< 0.001	0.002	0.948	−0.056–0.060
Gr_{IV}	0.551	0.569	< 0.001	0.400–0.737
Gr_{IV}/e'	0.704	4.667	< 0.001	3.289–6.045

Gr_{IV}/e' Apical intraventricular velocity gradient mitral annulus velocity ratio. Other abbreviations same as in Table 2

Intraventricular velocity distribution

In our study, we used VFM technology to visualize streamlines during the peak of LV rapid filling. Streamlines connect velocity vectors in a flow field and show the direction a fluid element is traveling in at given instant; a tangent to a streamline at any point is parallel to the fluid's instantaneous velocity at that point. When values of tangent velocities are plotted against the base-to-apex streamline's distance, the resulting plot gives information about velocity distribution along the streamline. Intraventricular velocity distribution pattern observed in this study during the peak of early diastole was concordant with our current physiological understanding of intraventricular fluid dynamics [16, 17] with increment of velocities in approximately first third and decrease of velocities in distal two thirds of LV. Increment part was characterized by two peaks, first coinciding with passage through the mitral valve orifice at the leaflet tips level and the second with the passage through the vortex ring. At LV level the strong toroidal vortex surrounding the central inflow core encroaches on the area available for

Table 3 Correlation of selected intraventricular velocities and intraventricular velocity gradient with conventional echocardiographic parameters

	V_{max}		V_{exit}		V_{apex}		Gr_{IV}	
	r	p	r	p	r	p	r	p
LAVI	0.353	< 0.001	0.429	< 0.001	0.023	0.801	0.545	< 0.001
E	0.714	< 0.001	0.728	< 0.001	0.375	< 0.001	0.643	< 0.001
E/A	0.706	< 0.001	0.663	< 0.001	0.376	< 0.001	0.483	< 0.001
e'	−0.054	0.560	−0.241	0.008	−0.003	0.977	−0.447	< 0.001
E/e'	0.580	< 0.001	0.709	< 0.001	0.260	0.004	0.751	< 0.001
TR velocity	0.635	< 0.001	0.660	< 0.001	0.327	0.005	0.651	< 0.001

exit at the exit of the vortex, *Gr_{IV}* apical intraventricular gradient, *max* maximal velocity, *V* velocity. Other abbreviations same as in Table 1

inflow towards the apex. This encroachment increases the central jet velocities, and causes higher linear velocities occurring dipper and later in the cavity. Measuring maximal velocities in the centre of toroidal vortex ring is consistent with previous studies on animal and human models [18]. Distal two thirds of LV were characterized by first, an abrupt decrement of velocities at the exit of vortex ring followed by a steady uniform decrement from the mid-ventricle towards the apex.

Intraventricular velocity distribution in our study was significantly different between groups (Table 2). The biggest differences were observed at the base of LV (V_{base}) at the entrance (V_{enter}) and in the vortex ring (V_{max}) where ADD group had the highest, MDD the lowest and control group velocities in-between. Measured values logically correlated strongly with peak E velocities measured by conventional pulsed Doppler. However, differences in velocities in the apex were less intense, significantly different only between ADD and MDD group. Consequently, calculated Gr_{IV}, representing decrease in velocity along the streamline between exit of vortex channel and the apex was the highest in the ADD and the smallest in control group (Fig. 5 right). The observed difference was created due to big variability in V_{exit} and little variability in velocities in the apex. In the selected frame where maximal intraventricular velocity was identified and our measurements were obtained, apex velocities were not different between ADD and control group (14.4 ± 6.9 vs. 13.0 ± 5.3 cm/s, $p = 0.567$), despite V_{max} and V_{exit} being significantly higher in ADD group. We hypothesize that the demonstrated difference in Gr_{IV} between groups was mainly due to combination of intraventricular flow delay and grade of velocity deceleration. We understand our findings through the fact that in normal hearts, during early filling, suction causes pressure to fall with very little temporal delay reaching maximum velocity almost simultaneously along the LV long axis [19]. Actually, we were able to demonstrate the differences in intraventricular delay (Δt) by measuring time to peak base and to peak apex velocity (Fig. 3). Intraventricular delay was significantly higher in ADD compared to MDD and control group (53.7 ± 38.2 vs. 20.0 ± 6.8 vs. 5.8 ± 3.2 ms, $p < 0.001$). Interestingly, similar pattern of kinetic energy behaviour during early diastole was recently reported by Garg et all [20] using cardiovascular magnetic resonance 4D flow.

Association with LV filling pressure

Preserved diastolic suction facilitates rapid filling and lowers minimum LV pressure [21], thus acting as a compensatory mechanism to maintain low LV filling pressure even

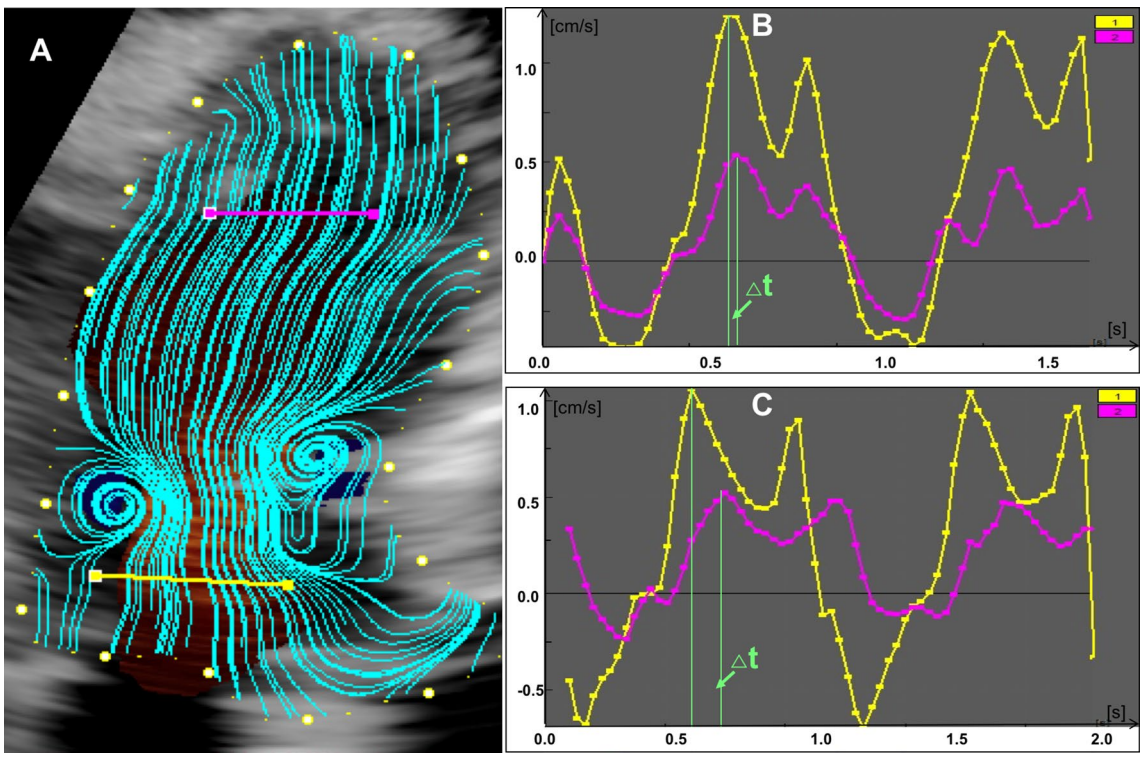

Fig. 3 Base-to-apex streamlines with sample cursors at the base (yellow) and in the apex (pink) of left ventricle (**a**). Velocity—time chart showing the delay between base (yellow line) and apex (pink line) peak velocity (Δt) for subject with normal diastolic function (**b**) and patients with restrictive left ventricular filling (**c**)

in situations of increased contractility. In case of altered relaxation and/or recoil forces, the LV needs to augment its filling pressure in order to maintain stroke volume [22]. The filling flow under these circumstances would encounter higher pressures as it moves downstream and would lose its velocity in a shorter distance. This has been described as a convective deceleration load and was linked to E/A ratio abnormalities, elevated LA pressure, acute and chronic heart failure and chamber dilatation [23, 24]. In fact, in our study Gr_{IV} parameter was strongly related to the E/e' ratio (Table 3) suggesting good association with non-invasive estimation of LV filling pressure (Fig. 4).

New Gr_{IV}/e' parameter

The interplay between factors determining LV filling is complex and force us to use many parameters to describe diastolic function. Combining flow mapping technology with conventional echocardiographic technique, we tried to integrate hemodynamic determinants of diastolic function within a single parameter. On one side, we demonstrated that Gr_{IV} is related to LV filling pressure; on the other, it is generally accepted that e' is associated with LV relaxation and is less dependent on LV load and as expected, in our population e' was significantly different among groups (Fig. 5 left). Finally, we corrected our new Gr_{IV} parameter for the effect of LV relaxation with e' conveying an integrated parameter Gr_{IV}/e' that could theoretically describe LV diastolic function.

In our study population, Gr_{IV}/e' emerged as the strongest independent predictor of the grade of diastolic dysfunction, being able to correctly categorize 70.4% of cases (Table 4, Fig. 6). On the other hand, all conventional parameters together could explain 79.5% of cases.

Intra- and interobserver variability

In addition, 10% of the post-processing measurements were repeated by an experienced VFM software user and an in-training cardiologist. The intra- and interobserver variability were excellent. This high reproducibility of measured parameters has the potential to be widely useful, since current assessment of diastolic dysfunction and LV filling pressures relies on multiple parameters and interobserver variability in usually high.

Clinical application

The ability to assess diastolic function with one parameter and only based on early diastole may allow easier and faster assessment of cardiac function and could provide additional information in response to pharmacological

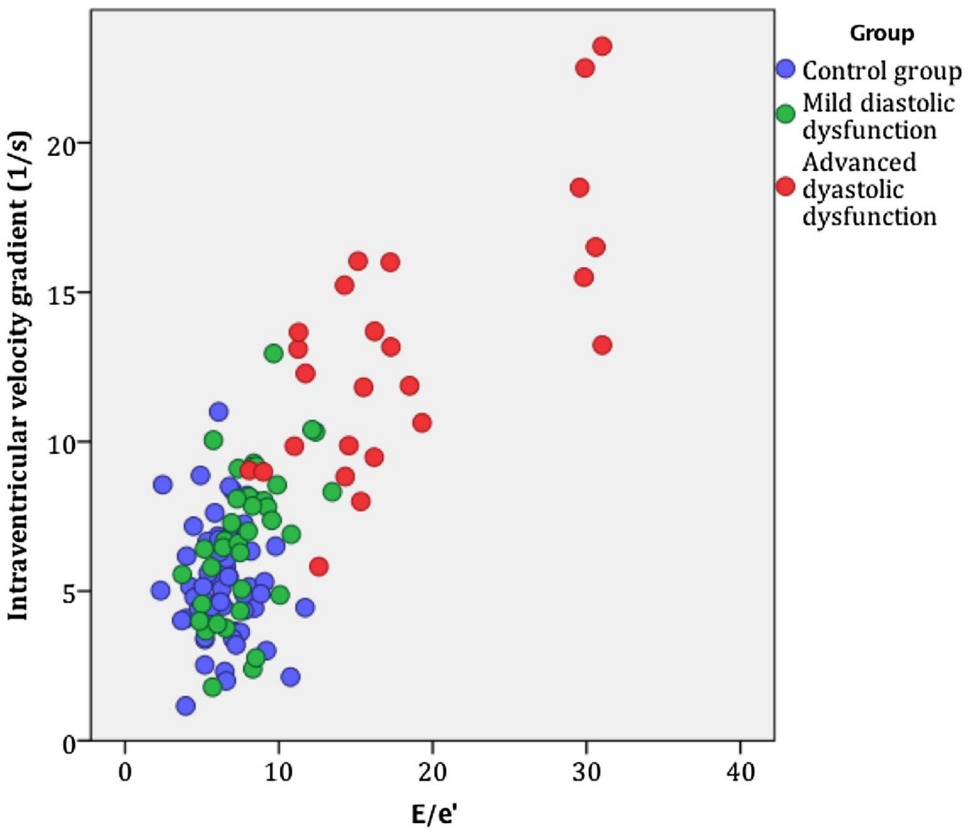

Fig. 4 Associations analysis of intraventricular velocity gradient obtained by vector flow mapping vs. marker of left ventricular filling pressure obtained by conventional echocardiography where blue dots represent control group, green dots patients with mild diastolic dysfunction and red dots patients with type II and III diastolic dysfunction

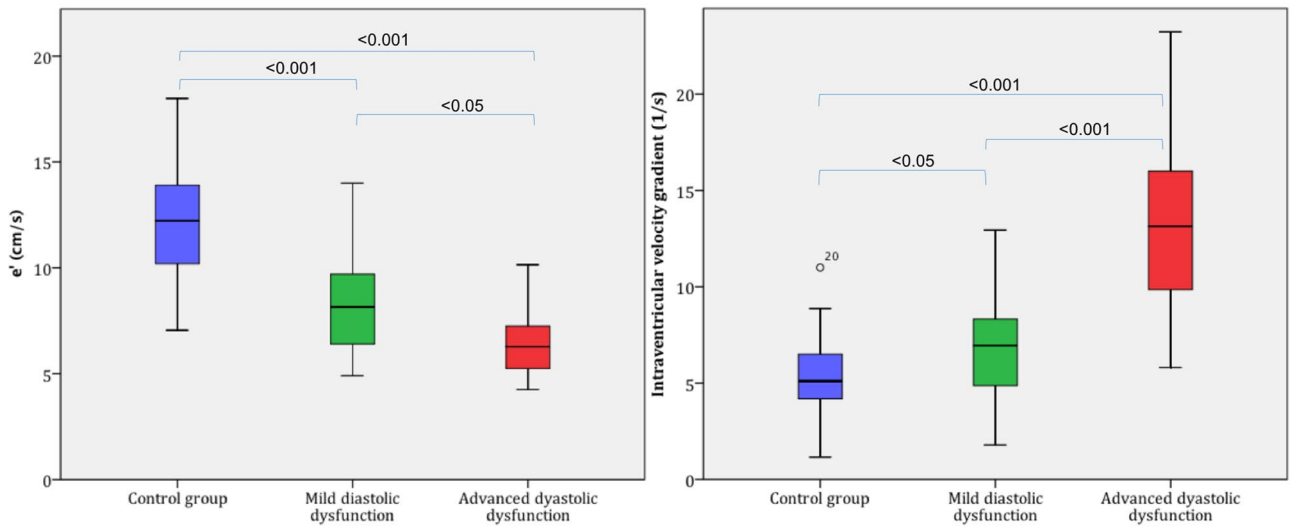

Fig. 5 Mean and standard error bars show the difference between groups for LV early diastolic average mitral annulus velocity (left) and intraventricular velocity gradient (right)

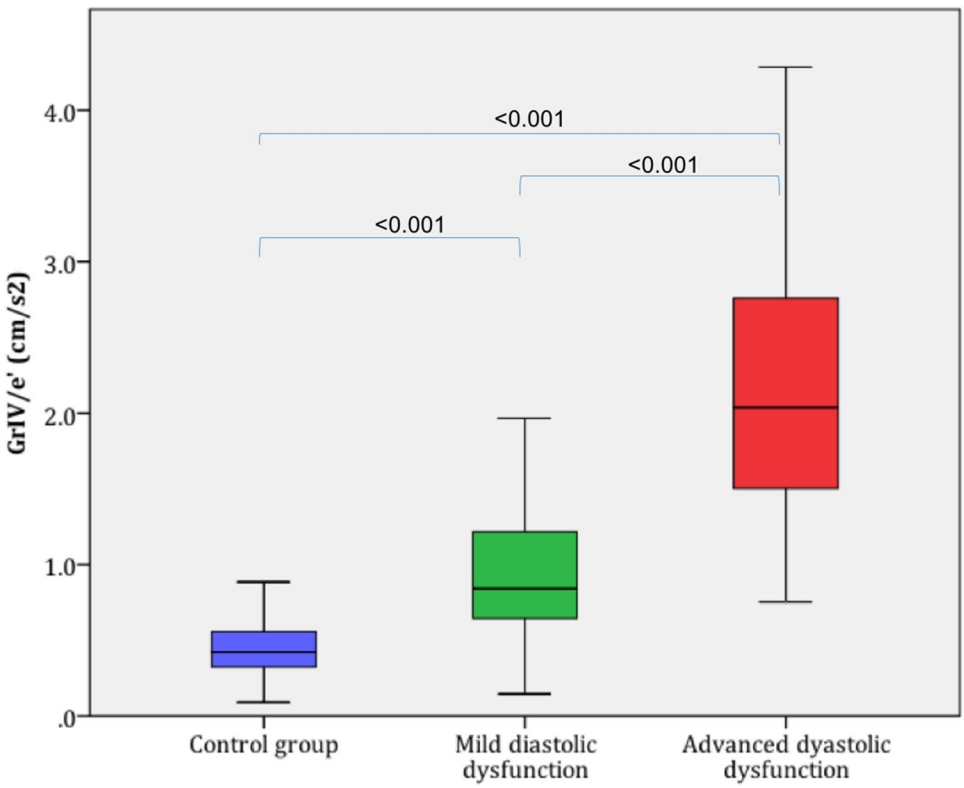

Fig. 6 Mean and standard error bars show the difference between groups for Intraventricular velocity gradient/mitral annulus early diastolic velocity ratio (Gr_{IV}/e')

treatment or in intraoperative assessment of surgical interventions. Moreover, its unique ability to assess diastolic function only by analysing early diastole might result as a crucial advantage in atrial fibrillation and other types of dysrhythmias. Further pre-clinical studies, where this technology is used in different haemodynamic conditions and simplification of semi-automated post-processing image software are needed to validate proposed parameters and enable faster translation of this technique into clinical practise.

Study limitations

Suboptimal visualization of LV walls for speckle tracking and very high transmitral velocity for 2D colour Doppler were the most important patient's characteristics that limited image processing. However, the first is a common limitation for echocardiography in general and the second could be resolved by excluding patients with mitral stenosis, besides software gives an option to manually correct aliasing colour turnover.

Definition of normal diastolic function in elderly is vague and controversial; thus, we decided not to balance groups for age and rather have a control group composed of consecutive healthy subjects with clearly normal diastolic function.

LV is a 3D structure, but our study utilizes a 2D vector field to describe intraventricular velocity distribution. This planar simplification may lead to inaccuracy in estimating velocity distribution. However, a simplified approach offers important advantages. First, our method is based on the continuity equation, there is a numerical benefit of operating with less parameters and reducing error of mathematic assumptions. Second, 2D can operate at high spatial and temporal resolutions that are necessary to accurately estimate intraventricular velocities.

Despite achieving good correlation of our new parameters with non-invasive indices of LV filling pressure, invasive measurements of LV filling pressures would be needed to validate this preliminary findings.

Conclusion

Intraventricular velocity gradient along the early diastolic filling streamline obtained by vector flow mapping could discriminate between groups with different levels of diastolic dysfunction with good inter- and intraobserver reliability and was associated with conventional echocardiographic indices of elevated LV filling pressure. Intraventricular velocity gradient, mitral annulus early diastolic velocity ratio could discriminate between groups with normal diastolic function, mild and advanced diastolic dysfunction and demonstrated the potential to be a novel single marker of diastolic dysfunction. Further studies are needed to evaluate the impact of medical decision based on intraventricular velocity distribution during early diastole obtained by vector flow mapping in different group of patients.

Compliance with ethical standards

Conflict of interest The authors declare that they have no conflict of interest.

References

1. Flachskampf FA, Biering-Sørensen T, Solomon SD, Duvernoy O, Bjerner T, Smiseth OA (2015) Cardiac imaging to evaluate left ventricular diastolic function. JACC Cardiovasc Imaging 8(9):1071–1093
2. Nagueh SF, Smiseth OA, Appleton CP, Byrd BF 3rd, Dokainish H, Edvardsen T et al (2016) Recommendations for the evaluation of left ventricular diastolic function by echocardiography: an update from the American Society of Echocardiography and the European Association of Cardiovascular Imaging. J Am Soc Echocardiogr 29(4):277–314
3. Kuwaki H, Takeuchi M, Chien-Chia Wu V, Otani K, Nagata Y, Hayashi A et al (2014) Redefining diastolic dysfunction grading: combination of E/A </=0.75 and deceleration time > 140 ms and E/epsilon' >/=10. JACC Cardiovasc Imaging 7(8):749–758
4. Bella JN, Palmieri V, Roman MJ, Liu JE, Welty TK, Lee ET et al (2002) Mitral ratio of peak early to late diastolic filling velocity as a predictor of mortality in middle-aged and elderly adults: the Strong Heart Study. Circulation 105(16):1928–1933
5. Mogelvang R, Sogaard P, Pedersen SA, Olsen NT, Marott JL, Schnohr P et al (2009) Cardiac dysfunction assessed by echocardiographic tissue Doppler imaging is an independent predictor of mortality in the general population. Circulation 119(20):2679–2685
6. Courtois M, Kovacs SJJ, Ludbrook PA (1988) Transmitral pressure-flow velocity relation. Importance of regional pressure gradients in the left ventricle during diastole. Circulation 78(3):661–671
7. Steine K, Stugaard M, Smiseth O (2002) Mechanisms of diastolic intraventricular regional pressure differences and flow in the inflow and outflow tracts. J Am Coll Cardiol 40(5):983–990
8. Pasipoularides A (2015) Mechanotransduction mechanisms for intraventricular diastolic vortex forces and myocardial deformations: part 1. J Cardiovasc Transl Res 8(1):76–87
9. Crandon S, Westenberg JJM, Swoboda PP, Fent GJ, Foley JRJ, Chew PG et al (2018) Impact of age and diastolic function on novel, 4D flow CMR biomarkers of left ventricular blood flow kinetic energy. Sci Rep 8(1):14436
10. Yotti R, Bermejo J, Antoranz JC, Desco MM, Cortina C, Rojo-Alvarez JL et al (2005) A noninvasive method for assessing impaired diastolic suction in patients with dilated cardiomyopathy. Circulation 112(19):2921–2929
11. Yamamoto K, Masuyama T, Tanouchi J, Naito J, Mano T, Kondo H et al (1995) Intraventricular dispersion of early diastolic filling: a new marker of left ventricular diastolic dysfunction. Am Heart J 129(2):291–299
12. Moller JE, Sondergaard E, Seward JB, Appleton CP, Egstrup K (2000) Ratio of left ventricular peak E-wave velocity to flow propagation velocity assessed by color M-mode Doppler echocardiography in first myocardial infarction: prognostic and clinical implications. J Am Coll Cardiol 35(2):363–370
13. de Knegt MC, Biering-Sorensen T, Sogaard P, Sivertsen J, Jensen JS, Mogelvang R (2014) Concordance and reproducibility between M-mode, tissue Doppler imaging, and two-dimensional strain imaging in the assessment of mitral annular displacement and velocity in patients with various heart conditions. Eur Heart J Cardiovasc Imaging 15(1):62–69
14. Itatani K, Okada T, Uejima T, Tanaka T, Ono M, Miyaji K et al (2013) Intraventricular flow velocity vector visualization based on the continuity equation and measurements of vorticity and wall shear stress. Jpn J Appl Phys 52:07HF16. https://doi.org/10.7567/JJAP.52.07HF16
15. Uejima T, Koike A, Sawada H, Aizawa T, Ohtsuki S, Tanaka M et al (2010) A new echocardiographic method for identifying

vortex flow in the left ventricle: numerical validation. Ultrasound Med Biol 36(5):772–788
16. Rodevand O, Bjornerheim R, Edvardsen T, Smiseth OA, Ihlen H (1999) Diastolic flow pattern in the normal left ventricle. J Am Soc Echocardiogr 12(6):500–507
17. Bellhouse BJ (1972) Fluid mechanics of a model mitral valve and left ventricle. Cardiovasc Res 6(2):199–210
18. Martinez-Legazpi P, Bermejo J, Benito Y, Yotti R, Perez Del Villar C, Gonzalez-Mansilla A et al (2014) Contribution of the diastolic vortex ring to left ventricular filling. J Am Coll Cardiol 64(16):1711–1721
19. Pasipoularides A, Shu M, Shah A, Tucconi A, Glower DD (2003) RV instantaneous intraventricular diastolic pressure and velocity distributions in normal and volume overload awake dog disease models. Am J Physiol Heart Circ Physiol 285(5):H1956–H1965
20. Garg P, Crandon S, Swoboda PP, Fent GJ, Foley JRJ, Chew PG et al (2018) Left ventricular blood flow kinetic energy after myocardial infarction—insights from 4D flow cardiovascular magnetic resonance. J Cardiovasc Magn Reson 20(1):61
21. Smiseth OA, Steine K, Sandbaek G, Stugaard M, Gjolberg T (1998) Mechanics of intraventricular filling: study of LV early diastolic pressure gradients and flow velocities. Am J Physiol 275(3):H1062–H1069
22. Kuecherer HF, Muhiudeen IA, Kusumoto FM, Lee E, Moulinier LE, Cahalan MK et al (1990) Estimation of mean left atrial pressure from transesophageal pulsed Doppler echocardiography of pulmonary venous flow. Circulation 82(4):1127–1139
23. Zhang W, Shmuylovich L, Kovacs SJ (2010) The E-wave delayed relaxation pattern to LV pressure contour relation: model-based prediction with in vivo validation. Ultrasound Med Biol 36(3):497–511
24. Pasipoularides A (2013) Evaluation of right and left ventricular diastolic filling. J Cardiovasc Transl Res 6(4):623–639